J.Phy.Ast.

Mehta PRESS

Full Paper

Journal of
Physics &
Astronomy

WWW.MEHTAPRESS.COM

Lizhong Ning[1]*, Bibo Ning[2], Weili Tian[3], Yoshifumi Harada[4], Hideo Yahata[5]

[1]Institute of Hydrodynamics, Xi'an University of Technology, South Jinhua Road, Xian 710048, (CHINA)
[2]College of Civil Engineering and Architecture, Jiaxing University, South Yuexiu Road, Jiaxing 314001, (CHINA)
[3]College of Fine Arts, Shanghai University, Shangda Road, Shanghai 200444, (CHINA)
[4]Department of Applied Physics, Faculty of Engineering, Fukui University, Bunkyo 3-9-11, Fukui 910, (JAPAN)
[5]Department of Materials, Science, Faculty of Science, Hiroshima University, Higashi-Hiroshima 739, (JAPAN)
E-mail: ninglz@xaut.edu.cn

Received: November 21, 2012
Accepted: December 30, 2012

*Corrresponding aurhor's
Name & Addess

Lizhong Ning
Institute of Hydrodynamics, Xi'an University of Technology, South Jinhua Road, Xian 710048, (CHINA)
E-mail: ninglz@xaut.edu.cn

Dynamics of Rayleigh-Benard convection in binary fluid mixture

Abstract

Convection in a thin, horizontal fluid layer heated from below is a typical model for studying nonlinear problem and chaos. The system is governed by the two-dimensional hydrodynamic equations. In this paper the SIMPLE algorithm was used to numerically solve the two-dimensional hydrodynamic equations of the coupled heat and concentration transfer as well as fluid flows. Our interest is focussed on the behavior of traveling wave convection along the nonlinear branch of subcritical bifurcation in a rectangular cell. Our simulation has reproduced the nonlinear phenomena observed in experiments such as counter-propagating wave (CPW), traveling wave (TW), localized traveling wave (LTW), undulation traveling wave (UTW) and stationary overturning convection (SOC) states appearing in the nonlinear branch of the subcritical bifurcation diagram and has interpreted their formation mechanism.

Key Words

Convection; Binary fluid mixture; Nonlinear phenomena; Traveling wave.

INTRODUCTION

Convection in a thin, horizontal fluid layer heated from below has been extensively studied during the last century. For a pure fluid, if the temperature difference applied across the fluid layer ΔT or the Rayleigh number R that is proportional to ΔT exceeds a certain threshold value ΔTc or R_c, the system undergoes a supercritical bifurcation at onset of convection to stationary overturning convection (SOC). However, for a binary fluid mixture such as water ethanol, the Soret effect leads to an additional control parameter besides the Rayleigh number R, namely, the separation ratio ψ, which measures the stabilizing ($\psi < 0$) or destabilizing ($\psi > 0$) effect of concentration gradients. Depending on ψ, the system which loses stability from a thermal conductive state gives rise to a SOC state which is the analogue of a pure fluid or to an oscillating convection state via a subcritical bifurcation, as shown in Figure 1. For negative values of ψ, the system undergoes a Hopf bifurcation at the onset of convection to a traveling wave (TW) state. It then evolves to several kinds of

fascinating patterns. The investigation on convection flows in a horizontal layer heated from below has mainly concentrated on experiments in a binary fluid layer with $\psi < 0$ in the last several years[5,12].

On the side of numerical simulations, using realistic no-slip, isothermal, impermeable lower and upper boundary conditions as well as realistic no-slip, adiabatic, impermeable lateral boundary conditions, Yahata obtained the counter propagating wave (CPW) and the localized traveling wave (LTW) states in a rectangular cell for ψ = -0.11 by numerically solving perturbation equations which are derived by the full hydrodynamic equations[15,16]. Using the same boundary conditions on the lower and upper plates in the cell as well as laterally periodic boundary conditions at both ends, Barten et al. simulated the LTW and the TW for ψ = -0.08 and ψ = -0.25 by using the finite difference method for the full hydrodynamic equations[1-4]. Using the simulation of he full hydrodynamic equations, we obtained the convective Patterns with defects[13,14]. These efforts were crowned with success. Using nonlinear perturbation equations, we also simulated the blinking traveling wave (BTW), LTW, double localized traveling wave (DLTW) states and their formation process[5-11]. However, up to now the study on the transition process of the traveling waves along the nonlinear branch in a rectangular cell is still not reported. In this paper our interest is focussed on the behavior in the transition of the TW convection patterns along the nonlinear branch in a rectangular cell of Γ = 12 for ψ = -0.11. Our numerical simulations have been performed by solving the two-dimensional hydrodynamic equations using the SIMPLE method.

THE GOVERNING EQUATIONS AND THE SIMPLE METHOD

Hydrodynamic equations and boundary conditions

Here, we consider a binary fluid layer heated from below under a homogeneous gravitational field, the flow above the onset of convection takes the form of straight rolls whose axes are parallel to two short side walls and perpendicular to two long side walls. If the effect of two long side walls or spatial variation along the roll axis is neglected, let x and z denote the Cartesian coordinates perpendicular to the roll axis with z directed upward. Within the framework of the Oberbeck-Boussinesq approximations, if lengths are further scaled by the thickness of the fluid layer d, time by d^2/k, the velocity field by k/d, temperature by $k\nu/\alpha gd^3$, concentration by $k\nu\gamma_2/\alpha gd^3D$, pressure by k^2/d^2, the hydrodynamic equations in dimensionless form can be written as

$$\nabla \cdot \delta U = 0 \quad (1)$$

$$\frac{\partial \delta U}{\partial t} + (\delta U \cdot \nabla)\delta U = \mathrm{Pr}\nabla^2 \delta U - \nabla\left(\frac{P}{\rho_0}\right) + (Ra\,\mathrm{Pr})[\delta T(1+\psi) + \delta\zeta]e_z \quad (2)$$

$$\frac{\partial \delta \mathrm{T}}{\partial t} + (\delta U \cdot \nabla)\delta T = \nabla^2 \delta T - LQ\psi\nabla^2\delta\zeta \quad (3)$$

$$\frac{\partial \delta\zeta}{\partial t} + (\delta U \cdot \nabla)\delta\zeta = L(1+Q\psi)\nabla^2\delta\zeta - \psi\nabla^2\delta T \quad (4)$$

Where the separation ratio $\psi = -(\frac{\beta}{\alpha})\cdot\frac{\kappa_T}{T_0}$, the Dufour number $Q = \frac{T_0}{C_p}\cdot\frac{\alpha}{\beta}\cdot\left(\frac{\partial\mu}{\partial C}\right)_{p,T}$, the Prandlt number $\mathrm{Pr} = \frac{\nu}{\kappa}$, the Lewis number $L = \frac{D}{\kappa}$, $\delta T = \frac{T-T_0}{\Delta T}$, $\delta C = \frac{\beta}{\alpha}\cdot\frac{C-C_0}{\Delta T}$, $\delta U = \frac{(u-u_0)d}{\kappa}$, $\frac{P}{\rho_0} = (\frac{P}{\rho_0} + gz)\cdot\frac{d}{\kappa}$, $\nu = \frac{\kappa T_D}{T_0}$, $\delta\zeta = \delta C - \psi\delta T$

Where u, T, C, ρ, g, C_p, t, κ, ν, D, μ denote the velocity vector, temperature, concentration, mass density, gravitational acceleration, specific heat, time, thermal diffusivity, kinemtic viscosity, concentration diffusion coefficient, chemical potential of the binary mixture respectively. κ_T is the coefficient relative to Dufour effect, T_0 donates the mean temperature below suffix 0 denotes the mean value corresponding to the physical quantities. For small deviations of T and C from the mean values T_0 and C_0, the equation of the state of the mass density can be written as

$$\rho = \rho_0[1 - \alpha(T - T_0) - \beta(C - C_0)] \quad (5)$$

Where the thermal expansion coefficient at constant pressure and concentration α and the solute expansion coefficient at constant temperature and pressure β are defined as

$$\alpha = -\frac{1}{\rho_0}\cdot\frac{\partial\rho(T,P,C_0)}{\partial T} \quad (6)$$

$$\beta = -\frac{1}{\rho_0}\cdot\frac{\partial\rho(T_0,P,C)}{\partial C} \quad (7)$$

The Dufour number Q and the Lewis number L for typical mixtures are about 10 times larger than in liquid mixtures, and the Dufour contribution is for the same fixed ψ about 10 times larger in gas mixtures than in liquid mixtures. Thus in gas mixtures Q can not be neglected. For the ethanol-water mixture, we shall neglect the Dufour effect in the following discussion.

Boundary conditions and initial conditions

To solve the governing equations, it is necessary to give reasonable boundary conditions. The walls are all rigid for the velocities and impermeable for the concentration current, that is

$\delta U = \delta W = \partial\delta\zeta / \partial z = 0$ at $z = 0,1$

$\delta U = \delta W = \partial\delta\zeta / \partial x = 0$ at $x = 0,\Gamma$

While the temperature is isothermal at z = 0,1 and adiabatic at $x = 0,\Gamma$, so that

$\delta T = 0.5$ at $z = 0$

$\delta T = -0.5$ at $z = 1$

$\partial \delta T / \partial x = 0$ at $x = 0, \Gamma$

The initial conditions are set by assuming that the flow takes the form of parallel rolls whose wavelength is just twice the thickness of the fluid layer and the initial rolls have small-amplitude envelopes which follows the shape of a Gaussian function whose peak is slightly asymmetrical.

Conductive solution

To simulate TW convection, we have solved the governing equations (1)-(4) by using the SIMPLE method. For this system, the conductive solutions can be written as

$$\delta U_{cond} = 0 \quad (8)$$

$$\delta T_{cond} = 0.5 - z \quad (9)$$

$$\delta C_{cond} = \psi(0.5 - z) \quad (10)$$

$$\delta \zeta_{cond} = 0 \quad (11)$$

$$(p / \rho_0)_{cond} = 0.5 \, Pr \, R(1 + \psi)(0.5 - z)^2 \quad (12)$$

Numerical method

The SIMPLE algorithm was used to numerically solve the governing equations consisting of the coupled heat and concentration transfer and fluid flows. The governing equations were solved in primitive variables in a two-dimensional staggered grids with an uniform spatial resolution $\Delta x = \Delta z = 1/20$ based on the control (finite) volume method. The power law scheme was used to treat the convective-diffusive terms in the discrete formulation. The discrete equations were solved by an iterative tri-diagonal matrix algorithm (TDMA). The time step Δt used in all calculations was 0.01, which represents 1% of the vertical relaxation time d^2/κ.

SIMULATIONAL RESULTS

Here we discuss the bifurcation behavior of the TW states in a rectangular cell in a binary mixture for $\psi = -0.11$, $L = 0.015$, $Pr = 18$. The conductive state loses its stability at the onset r_{osc}. Figure 1 displays the r-dependence of the Nusselt number N-1 and the amplitude of convection, where convection patterns depend on r, where r is a reduce Rayleigh number, $r = R/R_{co}$, R and R_{co} (= 1708) are a Rayleigh number and Rayleigh number at the onset of convection for pure fluid. Above the onset r_{osc}, the system evolves into the nonlinear TW state with a large amplitude. For our given parameters, the onset of the oscillatory instability is equal to 1.17. When r exceeds 1.17, a transient counter-propagating wave (CPW) is obtained. Figure 2 shows the counter-propagating wave state at r = 1.2. When we decrease r from 1.15 to 1.14 along the upper nonlinear branch, the TW state loses its stability. For $r > 1.15$, the TW state is stable. It persists over the range of $1.15 < r < 1.26$.

If r exceeds 1.26, an undulation TW appears in the system. Let us now consider the dynamical behavior in detail. When r is increased from 1.15 to 1.26, the traveling wave always maintain the identical direction of propagation and move to the right with the phase velocity, which decreases with an increase of r. When r is increased to 1.28, however, the right-going TW reverses the direction of propagation and begins to move to the left near t = 10. The TW states with the propagating direction of this type of "S" have been

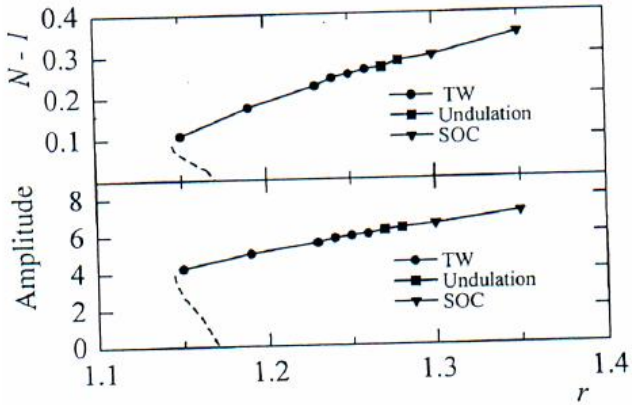

Figure 1 : Bifurcation diagrams of binary fluid convection in a rectangular cell (Γ = 12). The TW solution branch bifurcates backwards at $r_{osc} = 1.162$, and exists over the range from r = 1.145 to r = 1.26. The SOC is stable above $r_{osc} = 1.30$, and the undulation TW is located over the range r = 1.26 to r = 1.30. Upper figure: Nusselt number; lower figure: amplitude.

called as the undulation TW states. With further increasing r, the system evolves into the SOC state above r = 1.30, as shown in Figure 1.

Figure 3 The transition to the LTW, where the computation is continued from the final state at r = 1.2 after r has slightly decreased to 1.181. Figure 4 Time evolution of the stream function ψ in the LTW state at r = 1.183. Each block represents an isopleth of ψ in the space(x,z), where the red and the black lines correspond to the positive and negative values of ψ respectively. Time proceeds in the upward direction, and the time interval between two successive blocks is $\Delta t = 8(\nu / d^2)$.

Let us now try to understand the structure of the TW and the SOC states. Figures 5, 6 display the structure of the TW at r = 1.15 near the saddle of bifurcation branch and the structure of the SOC state at r = 1.3. Both velocity and temperature fields look like those in a pure fluid, but in the binary fluid mixture, the temperature field is slightly phase shifted relative to the vertical velocity field. The streamlines also are similar to those in a pure fluid. The velocity, temperature and

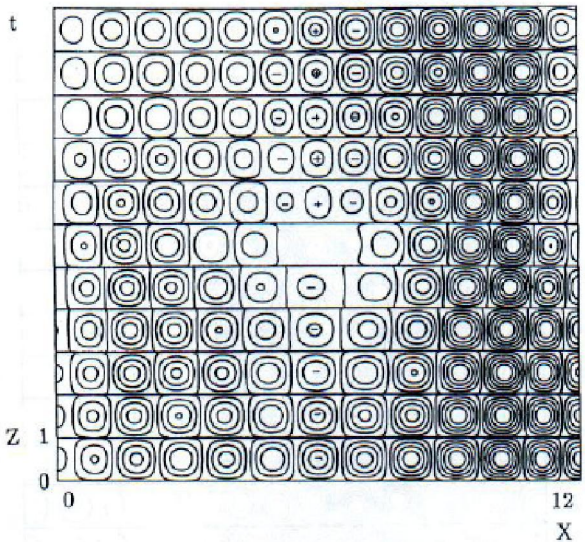

Figure 2 : Time evolution of the perturbation temperature field θ at r = 1.2, where the CPW is located near the center of the cell. Each block represents an isopleth of θ in the space(x,z), where the red and the black lines correspond to the positive and negative values of θ respectively. Time proceeds in the upward direction, and the time interval between two successive blocks is $\Delta t = 0.25(\nu / d^2)$.

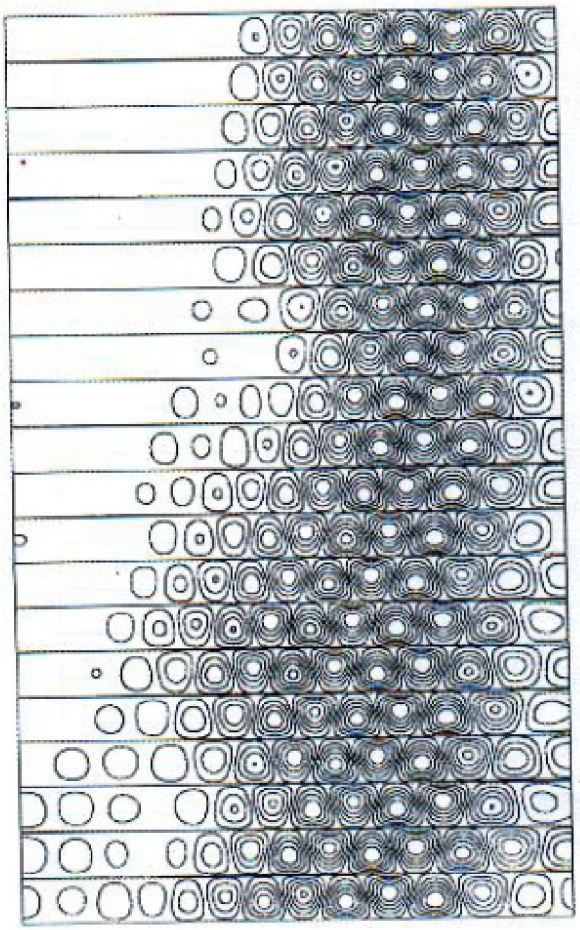

Figure 3 : The transition to the LTW, where the computation is continued from the final state at r = 1.2 after r has slightly decreased to 1.181. Time proceeds in the upward direction, and the time interval between the two successive blocks is $\Delta t = 8(\nu / d^2)$.

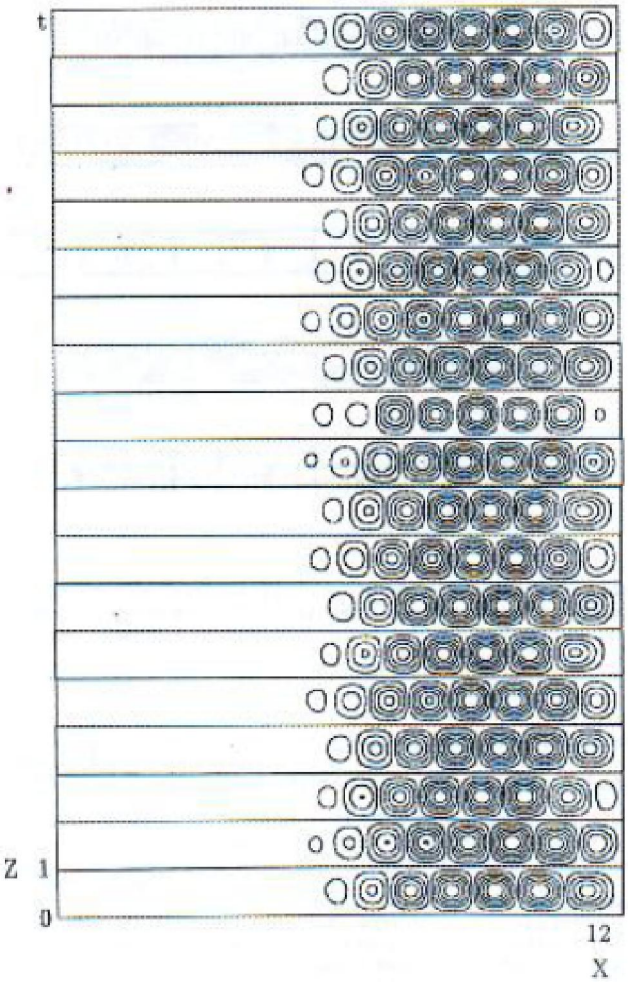

Figure 4 : Time evolution of the stream function ψ in the LTW state at r = 1.183. Each block represents an isopleth of ψ in the space(x,z), where the red and the black lines correspond to the positive and negative values of ψ respectively. Time proceeds in the upward direction, and the time interval between two successive blocks is $\Delta t = 8(\nu / d^2)$.

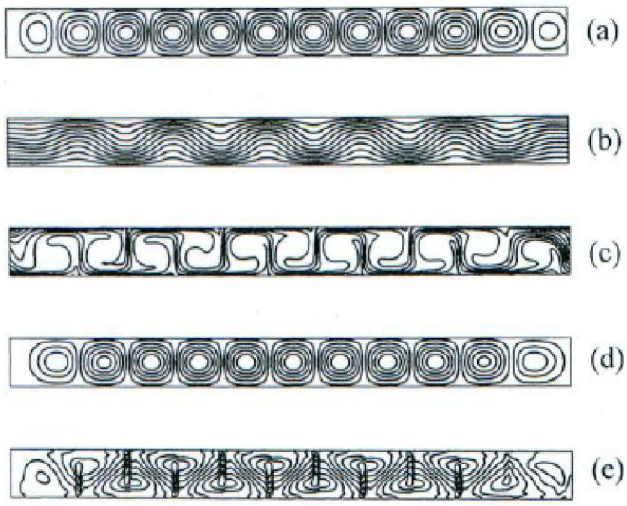

Figure 5 : The spatial patterns of the TW propagating to the right near the saddle of the bifurcation diagram at r = 1.19. (a) Vertical component of the velocity, (b) temperature δT, (c) concentration δC, (d) streamline, (e) side view shadowgraph intensities I(x,z).

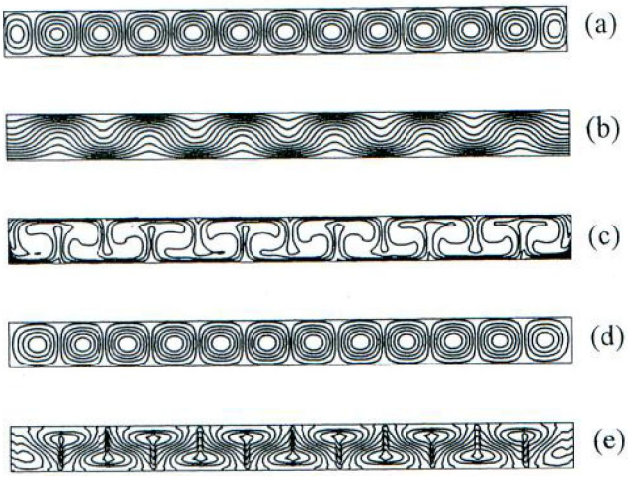

Figure 6 : The spatial of the SOC state at r = 1.35. (a) Vertical component of the velocity, (b) temperature δT, (c) concentration δC, (d) streamline, (e) side view shadowgraph intensities I(x, z).

streamline all are mirror symmetric around the centerline of rolls. The plume structure of the concentration fields in the TW state shown in figure 5. is different from that in SOC state shown in Figure 6. The plume in the SOC state locates at the position of maximal up and down flow, and is mirror symmetric. While in an TW state, the concentration jets alternatingly feed only the left or right turning rolls. The plumes are strongly bent into the respective rolls, and the resulting fine structure of concentration. The property of the sideview shadowgraph intensities in the TW state is different from that in the SOC state. In the SOC state Figure 6, the rolls constructed by contours of sideview shadowgraph intensities are mirror symmetry around the centerline of rolls. However, in the TW state, the contours of sideview shadowgraph intensities are bent and mirror symmetry around the centerline of rolls breaks due to an TW. It should been pointed out that the contours of the sideview shadowgraph intensities character the state of binary fluid convection as the concentration field.

CONCLUSION

To reveal the behavior in the transition of the convection patterns along the nonlinear branch of binary fluid convection confined in the rectangular cell with $\Gamma = 12$ for $\psi = -0.11$, we have solved the two-dimensional full hydrodynamic equations by using the SIMPLE method.

Our simulation has reproduced the nonlinear phenomena observed in experiments such as traveling wave (TW), counter-propagating wave (CPW), localized traveling wave (LTW), undulation traveling wave (UTW) and stationary overturning convection (SOC) states appearing in the nonlinear branch of the subcritical bifurcation diagram.

REFERENCES

[1] W.Barten, M.Lucke, W.Hort, M.Kamps; Fully developed traveling wave convection in binary fluid mixtures, Phys.Rev.Lett., **63**, 376 **(1989)**.

[2] W.Barten, M.Lucke, M.Kamps; Localized traveling wave convection in binary fluid mixtures, Phys.Rev.Lett., **66**, 2621 **(1991)**.

[3] W.Barten, M.Lucke, M.Kamps, R.Schmitz; Convection in binary fluid mixtures I. Extended traveling wave and stationary states, Phys.Rev.Lett., **E51**, 5636 **(1995a)**.

[4] W.Barten, M.Lucke, M.Kamps, R.Schmitz; Convection in binary fluid mixtures II. Localized traveling wave, Phys.Rev.Lett., **E51**, 5662 **(1995b)**.

[5] L.Z.Ning; Traveling wave convection in binary fluid mixture, Yushodo Book, 1999, **(1999)**.

[6] L.Z.Ning, Y.Harada, H.Yahata; Localized traveling wave convection in binary fluid convection, Prog.Theor.Phys., **96**, 669 **(1996)**.

[7] L.Z.Ning, Y.Harada, H.Yahata; Modulated traveling wave convection in binary fluid convection in an intermediate-aspect-ratio rectangular, Prog.Theor.Phys., **97**, 831 **(1997a)**.

[8] L.Z.Ning, Y.Harada, H.Yahata; Formation process of traveling wave with a defect in binary fluid convection, Prog.Theor.Phys., **98**, 551 **(1997b)**.

[9] L.Z.Ning, Y.Harada, H.Yahata; Competing instabilities and traveling wave convection in binary fluid mixture, in COMPLEXITY and DIVERSITY, E.R.Nakamura, (Ed); Springer, 132 **(1997c)**.

[10] L.Z.Ning, Y.Harada, H.Yahata; Dynamics of localized traveling wave convection in binary fluid mixtures, J.of Hydrodynamics, **10(2)**, 29 **(1998)**.

[11] L.Z.Ning, Y.Harada, H.Yahata; Numerical simulations of traveling wave convection in a weakly nonlinear regime, J.of Hydrodynamics, **12(2)**, 20 **(2000)**.

[12] L.Z.Ning; Rayleigh-Benard convection in a binary fluid mixture with and without lateral flows, Xi' an: Northwest A &F Univ Press, **(2006)**.

[13] L.Z.Ning, L.Yu, Z.Yuan, Y.Zhou; Evolution of traveling wave patterns along upper branch of bifurcation diagram in binary fluid convection. Sci.Chin.G, **39(5)**, 746 **(2009a)**.

[14] L.Z.Ning, X.Qi, Y.Zhou, L.Yu; Defect structures of Rayleigh-Benard traveling wave convection in binary fluid mixtures. Acta Phys.Sin-cn ED, **58(4)**, 2528 **(2009b)**.

[15] H.Yahata; Dynamics of convection in binary fluid mixtures, Prog.Theor.Phys.Supplement 99, 493 **(1989)**.

[16] H.Yahata; Traveling convection rolls in a binary fluid mixture, Prog.Theor.Phys., **85**, 933 **(1991)**.